

Investigation of Single-Pixel Imaging Using Recurrent Neural Network

Ikuo Hoshi¹, Tomoyoshi Shimobaba¹, Takashi Kakue¹, Tomoyoshi Ito¹

¹Graduate School of Engineering, Chiba University

Keywords: Single-Pixel Imaging, Deep Learning, Recurrent Neural Network

ABSTRACT

We propose a reconstruction method for single-pixel imaging. Recently, reconstruction methods using deep neural networks have been studied. However, these methods need much calculation. In this paper, we investigated to reconstruct images from a single-pixel device using a recurrent neural network and decrease the calculation amount.

1 INTRODUCTION

Single-pixel imaging is a unique technique in terms of using a single element photodetector. We show a schematic of the method in Fig.1. The method reconstructs two- or three-dimensional images from one-dimensional sequence data that are light intensity obtained by illuminating the object with specific patterns. This technique has various methods for the reconstruction process: for example, correlation-based methods called "ghost imaging" (GI) [1-4], methods using basis patterns such as Hadamard and Fourier bases [5], and optimization methods [6,7]. The methods [1-5] require a lot of measurement time to obtain better image quality and the methods [6,7] require the calculation time for the iterative optimization. For that reason, high-speed single-pixel imaging, such as using an FPGA [8], has been studied. In recent years, among them, reconstruction methods using deep neural networks [9,10] based on convolutional neural networks (CNNs) get much attention. The methods have an advantage that an image can be reconstructed with fewer measurements than previous methods. However, the methods have a disadvantage that the calculation amount is significant for high-speed imaging.

In this study, we proposed a recurrent neural network (RNN)-based reconstruction from a single-pixel device and verified the image quality and the calculation amount.

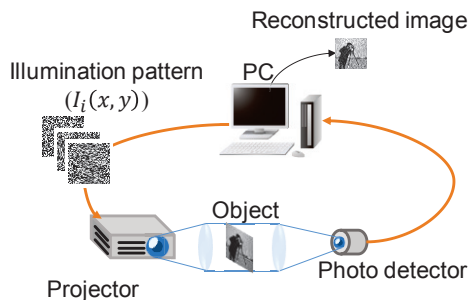


Fig. 1 Schematic of single-pixel imaging.

2 PROPOSED METHOD

An RNN is one of deep neural networks. We show a schematic of an RNN structure in Fig.2. An RNN has some features. For example, it has a recursive network structure. Compared to CNNs, an RNN can treat time series data because of this feature and can decrease network parameters while keeping deep layers. Therefore, for single-pixel imaging, an RNN has the possibility of reconstruction with fewer measurements than other methods without increasing the calculation amount.

$x(t)$: Input layer $h(t)$: Hidden layer $y(t)$: Output layer

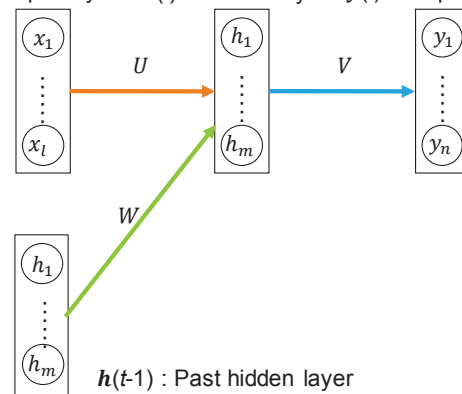


Fig. 2 Schematic of RNN.

In fig.2, $x(t)$, $h(t)$, and $y(t)$ represent the values of the input layer, hidden layer, and output layer at time t . Let U be the weight between the input layer and hidden layer, V be between the hidden layer and output layer, and W be the past hidden layer and current hidden layer. We show a mathematical model of the hidden layer in Eqs. (1) and (2). We show a mathematical model of the output layer in Eqs. (3) and (4).

$$p(t) = \mathbf{U}x(t) + \mathbf{W}h(t-1) + \mathbf{b} \quad (1)$$

$$h(t) = f(p(t)) \quad (2)$$

$$q(t) = \mathbf{V}h(t) + \mathbf{c} \quad (3)$$

$$y(t) = g(q(t)) \quad (4)$$

The biases to the hidden layer and output layer are \mathbf{b} and \mathbf{c} . $f(r)$ and $g(r)$ represent activation functions of the hidden layer and output layer. $p(t)$ is the output of the input layer before the activation function $f(r)$. Also, $q(t)$ is the output of the hidden layer before the activation

function $g(r)$. We adopted ReLU function as $f(r)$ and Leaky ReLU function as $g(r)$ because the output is an image data.

2.1 Dataset

We use “MNIST” as original images to verify the effectiveness of the proposed method. “MNIST” is image dataset including handwritten digits from zero to nine. The input data is one-dimensional time series data obtained by simulating the physical process in Fig.1. The output data is reconstructed images. We used the training data that consist of the time-series data and corresponding ground-truth image.

2.2 Single pixel imaging using RNN

We show a schematic of the proposed method in Fig.3. First, we obtain a time series data of object lights from an MNIST object by illuminating patterns. The calculation of an object light can be expressed as

$$S_i = \iint T(x, y) \cdot I_i(x, y) dx dy (i = 1, 2 \dots n), \quad (5)$$

where $I_i(x, y)$ is the light intensity distribution of the illumination patterns, and $T(x, y)$ denotes a distribution of object light. The subscript indicates the i -th pattern. Second, we input the time series data S_i of the object light to the RNN. Finally, we obtain a reconstructed image from the RNN.

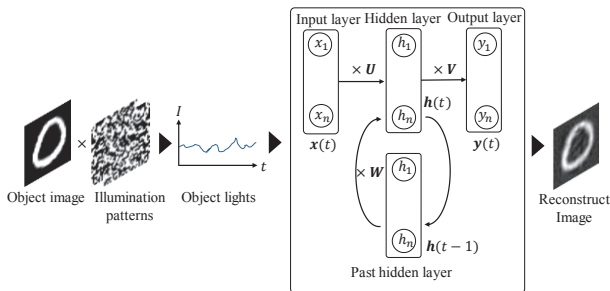


Fig. 3 Schematic of the proposed method.

3 RESULTS

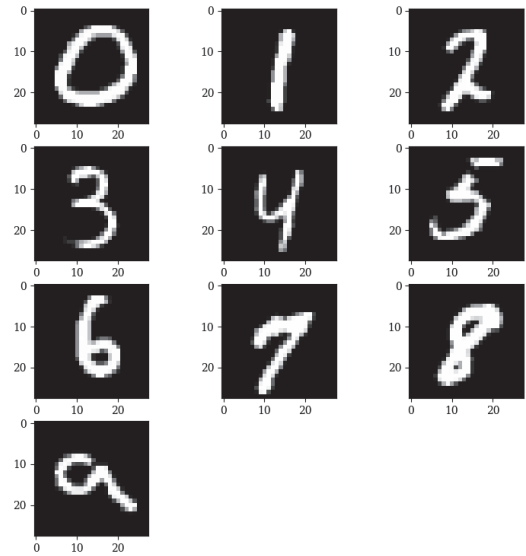
First, we show the comparison of a CNN calculation time and the RNN calculation time. For the computing environment, we used Intel Core™ i5 4690 (clock frequency 3.50 GHz) as the CPU, a memory of 8.0 GB, Microsoft Windows 10 education as the operating system, NVIDIA Geforce GTX 980 as the GPU, and Microsoft Visual Studio C++ 2015 as the compiler. The average calculation times for the CNN and the RNN are given in Table 1. There is no much difference between each calculation time.

Table 1 calculation time per image

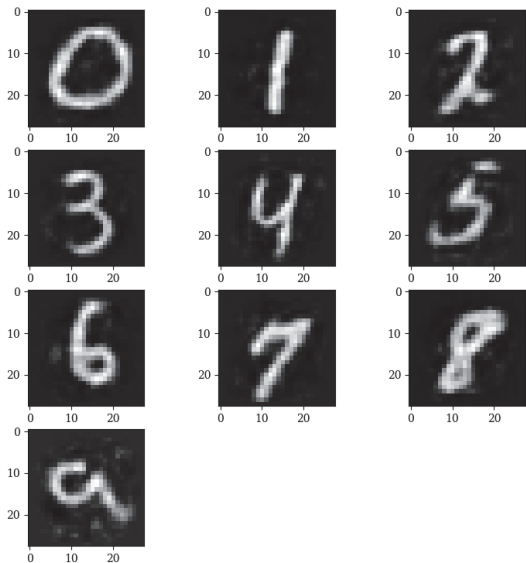
	CNN	RNN
Calculation time	86[μs]	95[μs]

Next, we show the comparison of original images and the reconstructed images using the proposed method in Fig. 4. The number of illumination patterns is 256. These

images are outputted as a grayscale with 8-bit. Figs. 4(a) and (b) show the original images and reconstructed images, respectively. As we can see from Fig.4, all the images could be reconstructed accurately. It shows that an RNN can reconstruct images from time-series data obtained with a single element detector.



(a) Original images.



(b) Reconstructed images.

Fig. 4 Original and reconstructed images.

Finally, we evaluated the image quality of reconstructed images from the RNN. Fig. 5 shows each reconstructed image using a conventional GI, a CNN, and the proposed method. Figs. 5(a)-(d) show an original image and the reconstructed images obtained by using the GI, a CNN and the proposed method. Table 2 shows the quantitative evaluation of Fig.5. We use peak signal-

to-noise ratio (PSNR) and structural similarity (SSIM) as the image quality index. The GI reconstruction does not have good image quality because the number of the illumination patterns is small. In contrast, the CNN and RNN can reconstruct better image quality even though the number of the illumination patterns is the same as the GI method. In addition, the reconstructed image obtained by the RNN is better than that of the CNN. Considering that the calculation times for the RNN and CNN are almost the same, it shows the effectiveness of the proposed method.

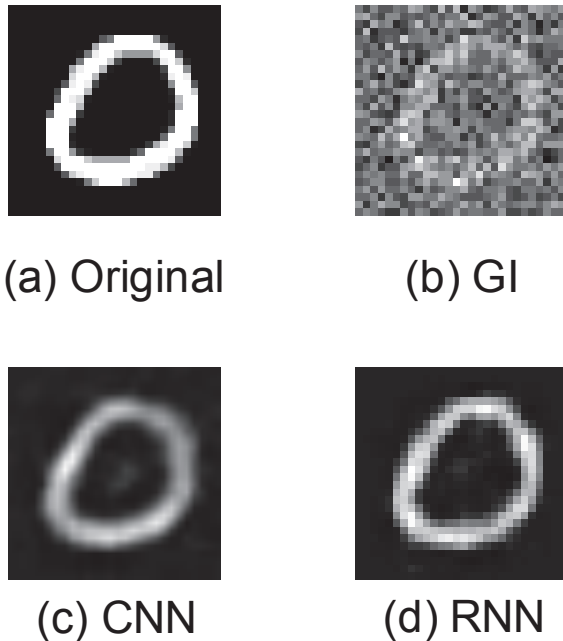


Fig. 5 evaluation image quality

Table 2 quantitative evaluation

	GI	CNN	RNN
PSNR (dB)	8.73	15.73	17.59
SSIM	0.30	0.80	0.88

4 CONCLUSIONS

We proposed a reconstruction method for single-pixel imaging using an RNN. We succeeded in reconstructing images using an RNN from time-series data. In future work, we try to reconstruct more complicated images with grayscale and implement our approach in a real optical system.

REFERENCES

- [1] T. B. Pittman, Y. H. Shon, D. V. Strekalov, and A. V. Sergienko, "Optical imaging by means of two photon quantum entanglement," *Phys. Rev. A* **52**, R3429 (1995).
- [2] F. Feeri, D. Magatti, A. Gatti, M. Bache, E. Brambilla, and L. A. Lugiato, "High-resolution ghost image and ghost diffraction experiments with thermal light," *Phys. Rev. Lett.* **94**, 183602 (2005).
- [3] J. H. Shapiro, "Computational ghost imaging," *Phys. Rev. A* **78**, 061802 (2008).
- [4] F. Ferri, D. Magatti, L. A. Lugiato, and A. Gatti, "Differential ghost imaging," *Phys. Rev. Lett.* **104**, 253603 (2010).
- [5] Z. Zhang, X. Wang, G. Zheng, J. Zhong, "Hadamard single-pixel imaging versus Fourier single-pixel imaging," *Opt. Express* **25**, 1617 (2017)
- [6] O. Katz, Y. Bromberg, and Y. Silberberg, "Compressive ghost imaging," *Appl. Phys. Lett.* **95**, 131110 (2009).
- [7] S. Ota, R. Horisaki, Y. Kawamura, M. Ugawa, I. Sato, K. Hashimoto, and K. Waki, "Ghost cytometry," *Science*, **360**(6394), 1246-1251 (2018).
- [8] I. Hoshi, T. Shimobaba, T. Kakue, and T. Ito, "Computational ghost imaging a field-programmable gate array," *OSA Continuum*, **2**, 1097-1105 (2019).
- [9] C. F. Higham, R. Murray-Smith, M. J. Padgett, and M. P. Edgar, "Deep learning for real-time single-pixel video," *Sci. Rep.* **8**, 2369 (2018).
- [10] T. Shimobaba, Y. Endo, T. Nishitsuji, T. Takahashi, Y. Nagahama, S. Hasegawa, and T. Ito, "Computational ghost imaging using deep learning," *Opt. Commun.* **413**, 147-151 (2018).